JOURNAL OF THEORETICAL
AND APPLIED MECHANICS
3, **36**, 1998

LOVE WAVE-INDUCED LIQUEFACTION IN A SATURATED SAND LAYER

RYSZARD STAROSZCZYK[1]

School of Mathematics, University of East Anglia, Norwich NR4 7TJ, United Kingdom
e-mail: R.Staroszczyk@uea.ac.uk

The paper is concerned with the plane strain problem of Love wave propagation through a water-saturated sand layer overlying an elastic half-space. Dynamic loads, induced by the wave passage, generate irreversible strains in the soil matrix, giving rise to the development of excess pore water pressures and subsequent reduction of the soil effective stresses, which in an extreme case can lead to the soil liquefaction. The process of pore pressure generation is analysed within the framework of compaction theory of saturated granular media. Results of numerical calculations, carried out by means of the finite element method, illustrate the evolution of pore pressures and the development of liquefaction in the subsoil, as well as the changes in the free surface displacements.

Key words: Love wave, saturated sand, soil liquefaction

1. Introduction

The phenomena of pore pressure generation and liquefaction, which can occur under certain conditions in fluid-saturated soils, are the subject of interest in several branches of science and engineering, including geophysics, civil and off-shore engineering, and the oil industry. The research in this field was initiated in the 1960s, following the Niigata (1964) and Alaska (1964) earthquakes, during which several examples of extensive soil liquefaction, leading to severe damages to buildings, were observed. The studies on the subject were

[1] On leave from the Institute of Hydroengineering of the Polish Academy of Sciences in Gdańsk

intensified in the 1970s, when large-scale marine structures subjected to water wave action were constructed in shelf regions on soils susceptible to liquefaction. It is also believed that the phenomena of pore pressure generation and liquefaction are the main reasons initiating underwater landslides, observed in several parts of the world (Syvitski and Schafer, 1990). On a smaller scale, soil liquefaction can develop in saturated sands during pile driving, or following the use of explosives (Studer and Kok, 1980).

Due to the complexity of the problem, associated with the two-phase nature of the medium, it seems that, despite considerable research efforts, there is still no well established theory, which could adequately describe the mechanical response of saturated soils to dynamic loads. So far, a number of theoretical models have been proposed (cf Martin et al., 1975; Seed et al., 1976; Finn et al., 1977; Ghaboussi and Dikmen, 1978; Martin and Seed, 1979; Nemat-Nasser and Shokooh, 1979; Zienkiewicz et al., 1982; Berrill and Davis, 1985; Law et al., 1990), which differ in the constitutive laws adopted for the modelling of the saturated soil, and include non-linear elasticity, elastoplasticity, viscoplasticity and plasticity. Plasticity theory has been the major approach, and various formulations regarding the soil response inside a yield surface, a yield condition, and a flow rule have been explored – many such examples can be found in the book by Pande and Zienkiewicz (1982). The classical plasticity models have been successfully applied to reproducion of the soil behaviour observed in experiments carried out in simple deformation configurations. In general, however, plasticity models give rise to very complex numerical problems, particularly in wave propagation analyses, in which moving interfaces that separate regions of distinct constitutive response occur. Another disadvantage of plasticity models is due to the use of non-associated flow rules, which leads to ill-posed problems, as it was pointed out by Schaeffer (1990).

In order to avoid the mathematical and numerical difficulties associated with the application of plasticity models to dynamic problems, other approaches, which do not require the concept of a yield surface, have been proposed. In these theories it is assumed that irreversible strains develop gradually and continuously during all loading, as opposed to classical plasticity in which plastic flow is started abruptly after a yield point has been reached. An example of such an approach is the endochronic theory formulated by Valanis (1971), and then extended by Bažant and Krizek (1976), Valanis and Read (1982), Bažant et al. (1983), Valanis and Peters (1991). Another alternative model, which avoids the notion of a yield surface, is the theory of compaction propo-

sed by Morland and Sawicki (1983, 1985), with a more rigorous generalisation by Morland (1993). In this theory, saturated sand is treated as a mixture of two immiscible constituents, skeleton grains and pore liquid, whose motion is coupled by diffusive forces of Darcy's type. In the model, reversible (elastic) and irreversible (inelastic) deformations are distinguished. The former are described by means of hypoelastic relations, while the latter, irreversible strains, are governed by evolutionary laws. These laws relate permanent volume compaction and shear settlement rates to the total strain history and the current deviatoric state.

In the present paper, the compaction theory of granular materials is utilised in order to analyse the pore pressure generation and liquefaction phenomena in a saturated sand layer subjected to seismic loads induced by Love surface waves. To date, when analysing the effects of earthquakes on saturated soils, the attention has been confined to either shear waves propagating upwards or Rayleigh surface waves, and a number of papers have been devoted to this subject, cf Seed et al. (1976), Gazetas and Yegian (1979), Zienkiewicz et al. (1982), Sawicki and Morland (1985), Sawicki and Staroszczyk (1995), Staroszczyk (1996). Despite an apparent similarity of the Rayleigh and Love surface wave propagation problems, there is a significant difference in particle motions and stress patterns induced by the two types of waves. While the former, Rayleigh waves, generate elliptic motions and both normal and shear stresses in the medium, the latter, Love waves, generate linear (horizontal) motions and shear stresses only. Since the phenomena of sand compaction, and hence pore pressure generation and liquefaction, strongly depend on the soil shear strains, these differences in stress patterns can affect, as already indicated by Gazetas and Yegian (1979), the soil liquefaction potential. It follows, therefore, that the problem of Love wave propagation in saturated sands deserves more attention than it has been given so far.

Relatively few papers, compared to the Rayleigh waves analyses, have dealt with Love wave propagation in two-phase media (cf Deresiewicz, 1961; Chakraborty and Dey, 1982; Chattopadhyay et al., 1986; Kończak, 1989), and none of them was concerned with the pore pressure generation and liquefaction phenomena. The present work attempts to fill this gap. Considerations are restricted to the plane strain problem of small and harmonic in time deformations. Numerical results, obtained by the use of the finite element method, show the time history of the excess pore pressure build-up, the liquefaction development within the sand layer profile, and changes in the free surface displacements.

2. Governing equations

We consider the propagation of SH waves travelling along a free surface of a semi-infinite medium. These waves consist of horizontally polarized disturbances perpendicular to the direction of propagation, decaying exponentially with distance from the free surface. It is well known that such waves cannot occur in a homogeneous elastic half-space (Achenbach, 1973). However, strong transverse motions are usually observed during earthquakes, and the existence of SH waves has been one of the first established facts of seismology. A theoretical explanation of these waves was provided by Love in 1911 (Ewing et al., 1957), who analysed the propagation of simple harmonic waves in a homogeneous elastic layer of uniform thickness, overlying a homogeneous and isotropic elastic half-space of a different material. Love showed that SH waves can occur only if the shear wave velocity in the upper stratum is less than that in the half-space, and that these waves are dispersive (in contrast to Rayleigh waves which are not dispersive). In the present analysis the upper layer is assumed to be inhomogeneous and transversely isotropic about the vertical, and consists of a liquid-saturated sand deposit, whose inhomogeneity varies with depth (Fig.1).

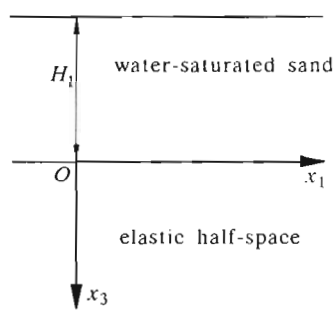

Fig. 1. Water-saturated sand layer underlain by an elastic half-space

We deal with the problem in which the dynamic loads are excited by earthquakes, i.e. the phenomena of a relatively short duration, usually not exceeding one minute. Since the soil liquefaction process can develop only in saturated sands of low permeability, it can be supposed that no significant drainage of the pore liquid takes place over such short time scales. Therefore one can assume that there is no motion of the pore fluid relative to the soil matrix, and hence the medium can be regarded as a single-phase solid whose displacement field is described by means of a single, common for the two phases, displacement vector $\boldsymbol{u}$.

In the adopted Cartesian coordinates $Ox_1x_2x_3$ (Fig.1), with the x_3-axis directed downward and the free surface at $x_3 = -H_1$, it is assumed that the time harmonic Love wave propagates in the positive x_1-direction, and the associated displacement field is described by

$$u(x_1, x_3, t) = u_0(x_3) \exp[\mathrm{i}(\omega t - kx_1)] \tag{2.1}$$

where

- u – particle displacement in the x_2-axis direction
- k – wavenumber
- ω – angular frequency
- t – time.

The function $u_0(x_3)$, the amplitude of oscillations, is required to satisfy the boundary conditions of zero shear stress σ_{32} at the free surface $x_3 = -H_1$ and zero displacement u as $x_3 \to \infty$. Accordingly,

$$\sigma_{32}(x_1, -H_1, t) = 0 \qquad \lim_{x_3 \to \infty} u(x_1, x_3, t) = 0 \tag{2.2}$$

furthermore, displacement and stress continuity at the interface $x_3 = 0$ are required.

Cyclic shear stresses, induced by the Love wave passage, give rise to irreversible rearrangements in the sand granular structure, which leads to pore volume decrease. The latter results in an increase in the pore fluid pressure, which in turn leads to a decrease in the mean effective pressure in the sand skeleton and subsequent loss of the subsoil shear strength. In the extreme case of near-zero effective pressures, the sand becomes a mobile suspension of loose grains and is said to have liquefied. Following Morland and Sawicki (1983), it is convenient to decompose the soil matrix strain $\boldsymbol{\varepsilon}$ into the reversible (elastic) and irreversible (compaction) parts, $\boldsymbol{\varepsilon}^e$ and $\boldsymbol{\varepsilon}^c$, respectively

$$\boldsymbol{\varepsilon} = \boldsymbol{\varepsilon}^e + \boldsymbol{\varepsilon}^c \tag{2.3}$$

and also to divide the strain tensor into a deviatoric part $\hat{\boldsymbol{\varepsilon}}$ and an isotropic part ε

$$\boldsymbol{\varepsilon} = \hat{\boldsymbol{\varepsilon}} + \frac{1}{3}\varepsilon \mathbf{I} \qquad \varepsilon = \operatorname{tr}\boldsymbol{\varepsilon} = \varepsilon^e + \varepsilon^c \tag{2.4}$$

where $\mathbf{I}$ is the unit tensor. The analogous partitions for the elastic and compaction strains are

$$\boldsymbol{\varepsilon}^e = \hat{\boldsymbol{\varepsilon}}^e + \frac{1}{3}\varepsilon^e \mathbf{I} \qquad \boldsymbol{\varepsilon}^c = \hat{\boldsymbol{\varepsilon}}^c + \frac{1}{3}\varepsilon^c \mathbf{I} \tag{2.5}$$

The total stress $\boldsymbol{\sigma}$ is decomposed into a deviatoric stress $\widehat{\boldsymbol{\sigma}}$ and a mean pressure p

$$\boldsymbol{\sigma} = \widehat{\boldsymbol{\sigma}} + p\mathbf{I} \qquad p = \frac{1}{3}\operatorname{tr}\boldsymbol{\sigma} \tag{2.6}$$

Here, the soil mechanics convention that strains and stresses are defined positive in compression is adopted. The total pressure p is a sum of partial pressures p^s in the solid matrix and p^f in the pore fluid

$$p = p^s + p^f \tag{2.7}$$

The partial pressures are, in turn, related to the corresponding intrinsic (actual) pressures p^{s*} and p^{f*} in the two phases of the medium by means of the formula

$$p^s = (1-n)p^{s*} \qquad p^f = np^{f*} \tag{2.8}$$

where n is the volume porosity of the medium. It is assumed that the pore fluid does not support shear stresses, and hence the partial stress in the fluid is an isotropic pressure, and the partial deviatoric stress in the matrix is the total deviatoric stress. The intrinsic pressures p^{s*} and p^{f*} in both constituents of the medium are related to the corresponding intrinsic strains (dilatations) ε^{s*} in the sand skeleton and ε^{f*} in the pore liquid by

$$\varepsilon^{s*} = \kappa_s p^{s*} \qquad \varepsilon^{f*} = \kappa_f p^{f*} \tag{2.9}$$

where κ_s and κ_f are, respectively, the intrinsic matrix and pore fluid compressibilities. In fully undrained conditions, under which there is no fluid flux from the matrix, and hence the pore fluid mass is locally conserved, the total compression is a sum of the partial compressions ε^s and ε^f in both phases, thus

$$\varepsilon = \varepsilon^s + \varepsilon^f = (1-n)\varepsilon^{s*} + n\varepsilon^{f*} \tag{2.10}$$

which, in view of (2.9), and then (2.8), yields

$$\varepsilon = \kappa_s p^s + \kappa_f p^f \tag{2.11}$$

The elastic isotropic response of the two-phase medium is assumed to depend linearly on the partial pressures in both constituents, which can be expressed by the relation

$$\varepsilon^e = \alpha_1 p^s + \alpha_2 p^f \tag{2.12}$$

with α_1 and α_2 being elastic constants. These constants can be determined in terms of the free draining and undrained compressibilities, κ and κ_u respectively, by conducting measurements in isotropic pressure when compaction does

not occur, in a way analogous to that described by Biot and Willis (1957). In a free drained (jacketed) test the intrinsic pore fluid pressure is held zero, and the applied pressure p is supported by the solid matrix only, thus

$$p^f = 0 \qquad p^s = p \qquad \varepsilon = \varepsilon^e = \kappa p \tag{2.13}$$

In an undrained test there is no pore liquid flux from the matrix, and by definition

$$\varepsilon = \varepsilon^e = \kappa_u p \tag{2.14}$$

Now, on substituting Eqs (2.13) and (2.14) into Eq (2.12), and then using Eqs (2.7) and (2.11) with $\varepsilon^c = 0$, one can express the elastic constants α_1 and α_2 in terms of the four compressibilities κ, κ_u, κ_s and κ_f as follows

$$\alpha_1 = \kappa \qquad \alpha_2 = \kappa_f - (\kappa - \kappa_s)\frac{\kappa_f - \kappa_u}{\kappa_u - \kappa_s} \tag{2.15}$$

As irreversible compaction ($\varepsilon^c > 0$) develops under undrained conditions, then Eqs (2.11), (2.12) with the definitions (2.15) and (2.7) provide the formulae which relate the elastic compression ε^e and the pore fluid partial pressure p^f to the total pressure p and the irreversible compression ε^c

$$\varepsilon^e = \kappa_u p - \frac{\kappa - \kappa_u}{\kappa - \kappa_s}\varepsilon^c \qquad p^f = \frac{\kappa_u - \kappa_s}{\kappa_f - \kappa_s}\left(p + \frac{\varepsilon^c}{\kappa - \kappa_s}\right) \tag{2.16}$$

and the total compression $\varepsilon = \varepsilon^e + \varepsilon^c$ is given by

$$\varepsilon = \kappa_u p + \frac{\kappa_u - \kappa_s}{\kappa - \kappa_s}\varepsilon^c \tag{2.17}$$

The effective pressure $\overline{p}$, which is a measure of intergranular contact forces and considerably influences the shear response of the medium, is defined by

$$\overline{p} = p - p^{f*} = p - \frac{p^f}{n} \tag{2.18}$$

where use of Eq $(2.8)_2$ has been made. On substituting Eq $(2.16)_2$ into Eq (2.18), the effective pressure is given by the relation

$$\overline{p} = \overline{p}_e - p_g \tag{2.19}$$

where

$$\overline{p}_e = \left[1 - \frac{\kappa_u - \kappa_s}{n(\kappa_f - \kappa_s)}\right]p \qquad p_g = \frac{\kappa_u - \kappa_s}{n(\kappa_f - \kappa_s)(\kappa - \kappa_s)}\varepsilon^c \tag{2.20}$$

In the above formulae $\overline{p}_e$ is related to the mean total pressure p, which can either increase or decrease as densification takes place, while p_g, related to the irreversible (increasing) compaction ε^c, describes the excess pore fluid pressure developing in the medium as permanent granular rearrangement caused by shearing progresses. As follows from Eq (2.19), the excess pore pressure p_g gradually reduces the effective pressure $\overline{p}$ from its initial magnitude, $\overline{p}_0$ say, in the pre-compacted state, until the effective pressure state in the medium reaches the liquefaction condition $\overline{p} = 0$.

In soil mechanics it is commonly assumed that the four compressibilities satisfy the inequality $\kappa_s < \kappa_u < \kappa_f < \kappa$. Usually $\kappa_s \ll \kappa_u$ for saturated sands, and therefore the approximation $\kappa_s = 0$ is often applied, with which Eq $(2.20)_2$ simplifies to

$$p_g = \frac{\kappa_u}{n\kappa_f \kappa}\varepsilon^c \tag{2.21}$$

Sometimes it is also assumed that the undrained compressibility κ_u is related to the intrinsic pore fluid compressibility κ_f through $\kappa_u = n\kappa_f$, which leads to a further simplification

$$p_g = \frac{\varepsilon^c}{\kappa} \tag{2.22}$$

The above formula is the relation proposed by Martin et al. (1975), and has usually been applied in engineering applications, particularly in cases in which the undrained compressibility κ_u is not known.

The constitutive response of a saturated sand is described within the framework of the compaction theory for granular media (Morland, 1993). In this model the evolution of both irreversible compaction and shear strains is described in terms of a time-independent loading parameter ξ, which increases monotonically as shearing takes place, but remains constant when purely isotropic strains occur. This parameter, representing an accumulating deviatoric strain, is defined by

$$d\xi = \sqrt{\frac{1}{2}\,\mathrm{tr}\,(d\widehat{\boldsymbol{\varepsilon}})^2} = \sqrt{\frac{1}{2}(d\widehat{\varepsilon}_{ij})(d\widehat{\varepsilon}_{ij})} \tag{2.23}$$

Here the summation convention over repeated subscripts is applied. The current strain state in the medium is described with the help of the following scalar measure

$$\psi = \frac{1}{2}\,\mathrm{tr}\,(\widehat{\boldsymbol{\varepsilon}})^2 = \frac{1}{2}\widehat{\varepsilon}_{ij}\widehat{\varepsilon}_{ij} \tag{2.24}$$

which is the second deviatoric strain invariant. The elastic strains are determined by hypoelastic relations. The elastic compression ε^e is governed by Eq

$(2.16)_1$, which in differential form becomes

$$\frac{d\varepsilon^e}{d\xi} = \kappa_u \frac{dp}{d\xi} - \left(\frac{\kappa - \kappa_u}{\kappa - \kappa_s}\right)\frac{d\varepsilon^c}{d\xi} \tag{2.25}$$

although the rate form cannot be used during purely isotropic deformation when ξ remains constant. The elastic shear strains obey the hypoelastic shear law

$$2G(\bar{p})\frac{d\hat{\varepsilon}^e}{d\xi} = \frac{d\hat{\sigma}}{d\xi} \tag{2.26}$$

where the shear modulus G is assumed here to depend on the current state through the effective pressure $\bar{p}$ only, but in general G could also depend on other scalar measures such as the current deformation ε^c, or the deviatoric strain or stress tensor invariants.

The volume compaction ε^c and irreversible deviatoric shear strains $\hat{\varepsilon}^c$ are governed by evolutionary laws, which describe the progress of irreversible strains with the increasing loading parameter ξ by means of the following differential equations

$$\frac{d\varepsilon^c}{d\xi} = D(\varepsilon^c, \psi) \qquad \frac{d\hat{\varepsilon}^c}{d\xi} = T(\varepsilon^c, \psi)\hat{\varepsilon} \tag{2.27}$$

D and T are material functions which incorporate the dependence of the evolution rates on the current compaction ε^c and the current strain state measure ψ. In separable forms these functions are defined by

$$D = aR(\varepsilon^c)H(\psi) \qquad T = bR(\varepsilon^c)H(\psi)S(\psi)\psi^{-1/2} \tag{2.28}$$

where the functions R, H and S are dimensionless, positive and normalised by

$$R(0) = H(0) = S(0) = 1 \tag{2.29}$$

and a and b are positive constants. The four functions $G(\bar{p})$, $R(\varepsilon^c)$, $H(\psi)$ and $S(\psi)$ along with the constants a and b can be determined experimentally. In the present work we use the material functions which were obtained by correlating the selected model (B) from Morland et al. (1993) with data from tests carried out on the loose Leighton Buzzard sand. These functions are as follows

$$R(\varepsilon^c) = \exp\Big[-\sum_{m=1}^{5} r_m\Big(\frac{\varepsilon^c}{\varepsilon^*}\Big)^m\Big] \qquad \overline{H}(\overline{\psi}) = 1 + \sum_{m=1}^{5} h_m\Big(\frac{\overline{\psi}}{\varepsilon^*}\Big)^m$$

$$\overline{S}(\overline{\psi}) = 1 + \sum_{m=1}^{5} s_m\Big(\frac{\overline{\psi}}{\varepsilon^*}\Big)^m \qquad \overline{g}(\overline{p}) = g_0 + \sum_{m=1}^{5} g_m\Big(\frac{\overline{p}}{p^*}\Big)^m \tag{2.30}$$

where

$$H(\psi) = \overline{H}(\sqrt{3\overline{\psi}}) \qquad S(\psi) = \overline{S}(\sqrt{3\overline{\psi}})$$
$$\overline{g}(\overline{p}) = \frac{2}{3}\kappa G(\overline{p}) \qquad g_0 = \overline{g}(0) \tag{2.31}$$

and the normalising stress and strain units are

$$p^* = 10^6 \text{ Pa} \qquad \varepsilon^* = 0.01 \tag{2.32}$$

The coefficients of the functions (2.30) are shown in Table 1 (cf Morland and Staroszczyk, 1998).

Table 1. Compaction model coefficients

m	r_m	h_m	s_m	g_m
1	0.9850	0.2711	0.5667	0.7169
2	0.8938	0.5731	−4.9571	−0.1924
3	1.3061	0.4299	3.7706	0.0564
4	1.1841	0.7044	3.3436	−0.0004
5	0.8597	0.8735	−2.7056	0.0014

3. Compaction and pore pressure generation due to Love wave propagation

As a Love wave propagates in the x_1-direction through the sand layer (see Fig.1), shearing in the Ox_1x_2 and Ox_2x_3 planes takes place. There are no normal strains in the horizontal x_1- and x_2-directions, since only shear elastic deformations are induced by the SH wave. The only non-zero normal strain is that in the vertical direction x_3 due to the permanent settlement of the sand. Thus, the strain tensor $\boldsymbol{\varepsilon}$ and the associated deviatoric strain tensor $\widehat{\boldsymbol{\varepsilon}}$ are

$$\boldsymbol{\varepsilon} = \begin{bmatrix} 0 & \varepsilon_{12} & 0 \\ \varepsilon_{21} & 0 & \varepsilon_{23} \\ 0 & \varepsilon_{32} & \varepsilon_{33} \end{bmatrix} \qquad \widehat{\boldsymbol{\varepsilon}} = \frac{1}{3}\begin{bmatrix} -\varepsilon_{33} & 3\varepsilon_{12} & 0 \\ 3\varepsilon_{21} & -\varepsilon_{33} & 3\varepsilon_{23} \\ 0 & 3\varepsilon_{32} & 2\varepsilon_{33} \end{bmatrix} \tag{3.1}$$

It should be noted, however, that the elastic and compaction strain tensors $\boldsymbol{\varepsilon}^e$ and $\boldsymbol{\varepsilon}^c$ do have non-zero lateral components, but they balance one another

to maintain zero total strains. Hence, the elastic strain tensor $\boldsymbol{\varepsilon}^e$ and its deviatoric part $\widehat{\boldsymbol{\varepsilon}}^e$ have the forms

$$\boldsymbol{\varepsilon}^e = \begin{bmatrix} \varepsilon^e_{11} & \varepsilon^e_{12} & 0 \\ \varepsilon^e_{21} & \varepsilon^e_{11} & \varepsilon^e_{23} \\ 0 & \varepsilon^e_{32} & \varepsilon^e_{33} \end{bmatrix} \qquad \widehat{\boldsymbol{\varepsilon}}^e = \frac{1}{3}\begin{bmatrix} \varepsilon^e_{11} - \varepsilon^e_{33} & 3\varepsilon^e_{12} & 0 \\ 3\varepsilon^e_{21} & \varepsilon^e_{11} - \varepsilon^e_{33} & 3\varepsilon^e_{23} \\ 0 & 3\varepsilon^e_{32} & 2(\varepsilon^e_{33} - \varepsilon^e_{11}) \end{bmatrix} \tag{3.2}$$

and the compaction strain tensors $\boldsymbol{\varepsilon}^c$ and $\widehat{\boldsymbol{\varepsilon}}^c$ have analogous forms to $\boldsymbol{\varepsilon}^e$ and $\widehat{\boldsymbol{\varepsilon}}^e$, respectively.

The stress field consists of cyclic shear stresses generated by the wave passage and normal stresses due to the soil's own weight and the lateral constraints. While the vertical normal stress σ_{33} has a static character and does not change with time, the lateral normal stresses σ_{11} and σ_{22} vary with time as the material compacts. Accordingly, the components of the stress tensor $\boldsymbol{\sigma}$ and the associated deviatoric stress tensor $\widehat{\boldsymbol{\sigma}}$ are given by

$$\boldsymbol{\sigma} = \begin{bmatrix} \sigma_{11} & \sigma_{12} & 0 \\ \sigma_{21} & \sigma_{11} & \sigma_{23} \\ 0 & \sigma_{32} & \sigma_{33} \end{bmatrix} \qquad \widehat{\boldsymbol{\sigma}} = \frac{1}{3}\begin{bmatrix} \sigma_{11} - \sigma_{33} & 3\sigma_{12} & 0 \\ 3\sigma_{21} & \sigma_{11} - \sigma_{33} & 3\sigma_{23} \\ 0 & 3\sigma_{32} & 2(\sigma_{33} - \sigma_{11}) \end{bmatrix} \tag{3.3}$$

In the above strain and stress tensor forms (3.1) $\div$ (3.3) it has been assumed that there is lateral symmetry in the sand response throughout the densification process, expressed by $\varepsilon^e_{11} = \varepsilon^e_{22}$, $\varepsilon^c_{11} = \varepsilon^c_{22}$, and $\sigma_{11} = \sigma_{22}$. However, the latter relations hold only if such symmetry exists in the initial, pre-compacted state, cf Morland (1993). Here it is assumed that prior to the soil shaking the sand is in its natural state, i.e. all the stresses are entirely due to gravity, and therefore the above-postulated symmetry is the case in the present analysis.

In view of the deviatoric strain tensor components $(3.1)_2$, Eq (2.23) defining the loading parameter ξ yields

$$(d\xi)^2 = (d\varepsilon^e_{12} + d\varepsilon^c_{12})^2 + (d\varepsilon^e_{23} + d\varepsilon^c_{23})^2 + \frac{1}{3}(d\varepsilon_{33})^2 \tag{3.4}$$

and the state parameter ψ, defined by (2.24), becomes

$$\psi = \varepsilon^2_{12} + \varepsilon^2_{23} + \frac{1}{3}\varepsilon^2_{33} \tag{3.5}$$

The strain rate relations (2.25) $\div$ (2.27), governing the elastic and irreversible response of the saturated granular medium, provide the following incremental forms

$$
\begin{aligned}
&2d\varepsilon^e_{11} + d\varepsilon^e_{33} + B(2d\varepsilon^c_{11} + d\varepsilon^c_{33}) = \frac{2}{3}\kappa_u d\sigma_{11} \\
&d\varepsilon^e_{11} - d\varepsilon^e_{33} = \gamma d\sigma_{11} \\
&2d\varepsilon^c_{11} + d\varepsilon^c_{33} = Dd\xi \qquad\qquad d\varepsilon^c_{12} = T\varepsilon_{12}d\xi \\
&d\varepsilon^c_{23} = T\varepsilon_{23}d\xi \qquad\qquad d\varepsilon^c_{33} - d\varepsilon^c_{11} = T\varepsilon_{33}d\xi
\end{aligned} \tag{3.6}
$$

with

$$
B = \frac{\kappa - \kappa_u}{\kappa - \kappa_s} \qquad\qquad \gamma(\bar{p}) = \frac{1}{2G} \tag{3.7}
$$

and the lateral constraint is

$$
d\varepsilon_{11} = d\varepsilon^e_{11} + d\varepsilon^c_{11} = 0 \tag{3.8}
$$

From Eqs (2.19) and (2.20), the effective pore pressure increment is determined by

$$
d\bar{p} = \left[1 - \frac{\kappa_u - \kappa_s}{n(\kappa_f - \kappa_s)}\right]dp - \frac{\kappa_u - \kappa_s}{n(\kappa_f - \kappa_s)(\kappa - \kappa_s)}d\varepsilon^c \tag{3.9}
$$

where the mean pressure increment is

$$
dp = \frac{1}{3}(2d\sigma_{11} + d\sigma_{33}) = \frac{2}{3}d\sigma_{11} \tag{3.10}
$$

since $d\sigma_{33} = 0$ due to the assumed static character of the vertical stress σ_{33}.

Eqs (3.6) and (3.8) constitute a system of seven equations in seven increments $d\varepsilon^e_{11}$, $d\varepsilon^c_{11}$, $d\varepsilon^e_{33}$, $d\varepsilon^c_{33}$, $d\varepsilon^c_{12}$, $d\varepsilon^c_{23}$ and $d\sigma_{11}$. These equations can be rearranged to express the individual components in terms of the loading parameter increment $d\xi$, thus

$$
\begin{aligned}
&d\varepsilon^e_{11} = -d\varepsilon^c_{11} = \frac{1}{3}(T\varepsilon_{33} - D)d\xi \\
&d\varepsilon^e_{33} = \frac{1}{3(\lambda + 2\bar{g})}\{\lambda[(3A-1)D - 2T\varepsilon_{33}] + 2\bar{g}(T\varepsilon_{33} - D)\}d\xi \\
&d\varepsilon^c_{33} = \frac{1}{3}(D + 2T\varepsilon_{33})d\xi \qquad\qquad d\varepsilon^c_{12} = T\varepsilon_{12}d\xi \\
&d\varepsilon^c_{23} = T\varepsilon_{23}d\xi \qquad\qquad d\sigma_{11} = \frac{3\bar{g}}{2\kappa_u + \kappa}(T\varepsilon_{33} - AD)d\xi
\end{aligned} \tag{3.11}
$$

where

$$
A = \frac{\kappa_u - \kappa_s}{\kappa - \kappa_s} \qquad\qquad \lambda = \frac{\kappa}{\kappa_u} \tag{3.12}
$$

and $\overline{g}(\overline{p})$ is defined by Eq $(2.31)_3$. The total strain increment $d\varepsilon_{33}$ is given by

$$d\varepsilon_{33} = \frac{1}{\lambda + 2\overline{g}}(\lambda AD + 2\overline{g}T\varepsilon_{33})d\xi \tag{3.13}$$

Eqs (3.11), however, cannot be directly applied to determine the strain and stress increments, since the loading parameter increment $d\xi$, defined by Eq (3.4), involves the strain increments $d\varepsilon^c_{12}$, $d\varepsilon^c_{23}$ and $d\varepsilon_{33}$ yet to be found; i.e. we have a system of non-linear algebraic equations to solve. *In order to* solve this system, Eqs $(3.11)_4$, $(3.11)_5$ and (3.13) are substituted into Eq (3.4), which transforms the problem to the solution of a single non-linear algebraic equation for $d\xi$ of the form

$$(d\xi)^2\left(1-a_1^2-a_2^2-\frac{1}{3}a_3^2\right)-2d\xi\left(a_1 d\varepsilon_{12}+a_2 d\varepsilon_{23}\right)-\left[(d\varepsilon^e_{13})^2+(d\varepsilon^e_{23})^2\right]=0 \tag{3.14}$$

where

$$a_1 = T\varepsilon_{12} \qquad a_2 = T\varepsilon_{23} \qquad a_3 = \frac{1}{\lambda + 2\overline{g}}(\lambda AD + 2\overline{g}T\varepsilon_{33}) \tag{3.15}$$

and the elastic shear strain increments $d\varepsilon^e_{12}$ and $d\varepsilon^e_{23}$ are prescribed quantities, determined by the assumed wave field. In order to describe a valid constitutive response, Eq (3.14) has to yield a positive $d\xi$ for any strain and stress configuration. This imposes restrictions on a_1, a_2 and a_3, and hence on the compaction model response functions R, H, S and G and the constants a and b. Having determined $d\xi$ from Eq (3.14), all the strain and stress increments are given by Eq (3.11), and then the effective pore pressure increment $d\overline{p}$ is defined by Eqs (3.9) and (3.10).

4. Illustrations

The problem under consideration has been solved approximately by means of the finite element method; the main points of the applied numerical scheme are presented in the Appendix. Calculations have been carried out for a layer of water saturated sand of thickness $H_1 = 20\,\mathrm{m}$, overlying an elastic and impermeable bedrock. The following data, corresponding to the loose Leighton Buzzard sand, were used in the simulations: intrinsic sand density $\rho_s = 2.6 \cdot 10^3\,\mathrm{kgm}^{-3}$, initial porosity $n = 0.4$, earth pressure coefficient $K_0 = 0.5$ (needed to calculate the static mean pressure due to the soil own weight). The adopted compressibilities were: $\kappa = 0.62 \cdot 10^{-8}\,\mathrm{Pa}^{-1}$,

$\kappa_u = 0.2 \cdot 10^{-9}\,\mathrm{Pa}^{-1}$, $\kappa = 0.5 \cdot 10^{-9}\,\mathrm{Pa}^{-1}$, $\kappa_s = 0$. The sand shear modulus at $\overline{p} = 0$ was $G_0 = 8.25\,\mathrm{MPa}$ (which corresponds to $g_0 = 0.0341$) and, with the coefficients listed in Table 1, G varied approximately linearly within the range $0 \leqslant \overline{p} \leqslant 0.5\,\mathrm{MPa}$ to reach the magnitude 85 MPa at the upper limit. In the compaction model, apart from the coefficients included in Table 1, the constants $a = b = 0.1$ were used. A ground water table was assumed to lie 2 m below the free surface of the sand deposit. The bulk density and shear modulus of the bedrock were, respectively, $\rho_r = 2.2 \cdot 10^3\,\mathrm{kgm}^{-3}$ and $G_r = 100\,\mathrm{MPa}$. For numerical reasons, the underlying half-space was modelled as layer of the finite thickness $H_2 = 200\,\mathrm{m}$, which was about 3.4 times the initial Love wavelength. The simulations were conducted for a wave of angular frequency $\omega = 12.57\,\mathrm{rad/s}$, and it was assumed for simplicity that the wave energy was constant during an earthquake.

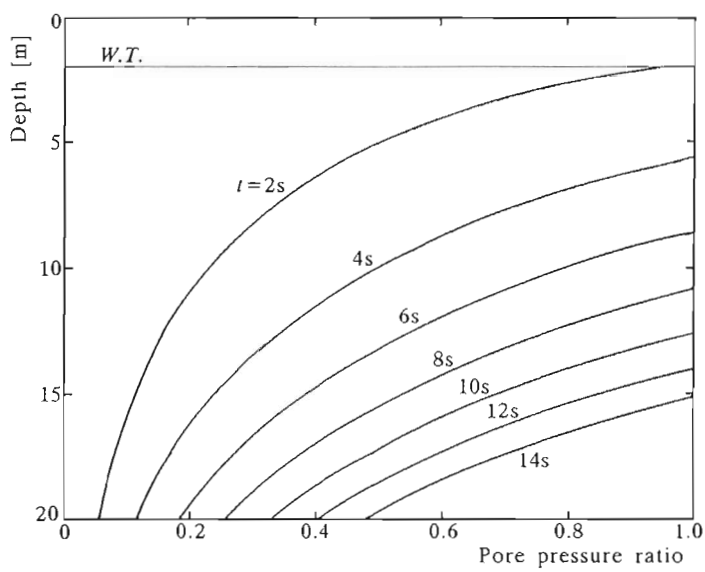

Fig. 2. Excess pore pressure generation history for different initial free surface acceleration amplitudes a_0 (W.T. denotes the ground water table level)

Fig.2 illustrates the variation of excess pore water pressures with time across the sand layer. The computed pore pressures p_g are normalised with respect to the sum of initial (static) effective pressure $\overline{p}_0$ and the pressure $\overline{p}_e$ generated during the sand compaction, i.e. the pressure ratios $p_g/(\overline{p}_0 + \overline{p}_e)$ are plotted. The presented results correspond to a wave which generates at the start of shaking a maximum ground acceleration $a_0 = 0.1g$ $(0.91\,\mathrm{ms}^{-2})$ at the free surface $x_3 = -H_1$. It is seen that the pore pressures develop in a very

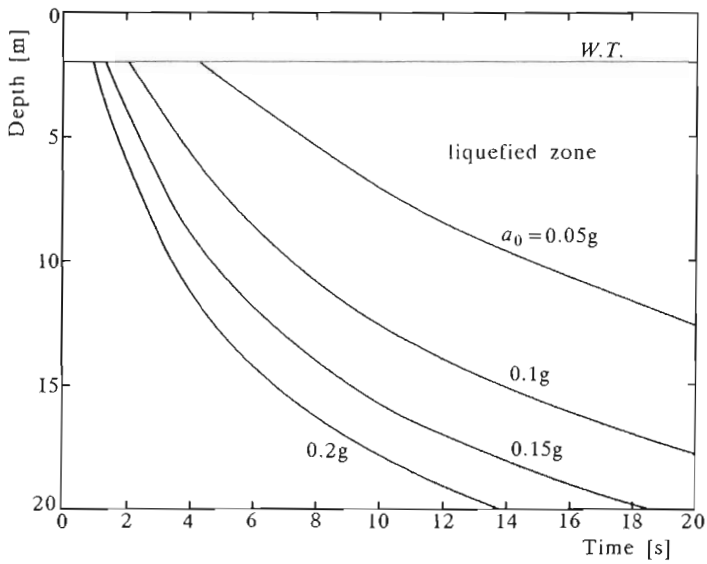

Fig. 3. Development of liquefaction for different initial free surface acceleration amplitudes a_0

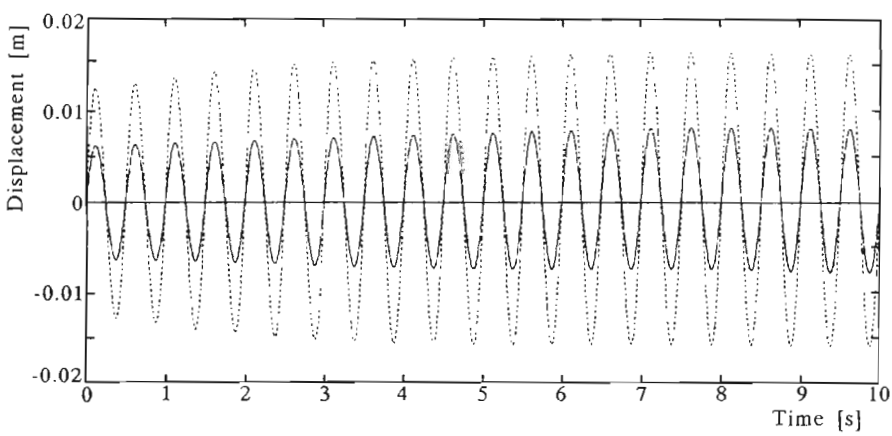

Fig. 4. Free surface horizontal displacement history for two initial acceleration amplitudes: (——) $a_0 = 0.1g$; (- - -) $a_0 = 0.2g$

regular manner throughout such an earthquake, and the liquefaction (which corresponds to the pore pressure ratio equal to unity) starts directly under the ground water table, where the soil shear strength, related to the effective pressure magnitude, is much smaller than at greater depths. The regular character of the pore pressures build-up differs from that in the Rayleigh wave case (cf Staroszczyk, 1996), in which the pore pressure development rates vary more dramatically, both in time and space.

In Fig.3, closely related to the previous one, the development of liquefied zones with time and depth is shown for different initial free surface acceleration amplitudes a_0. Again, it is observed that the range of liquefied soil increases monotonically with time. The highest rate of liquefaction occurs immediately after the onset of liquefaction near the water table, and the rate gradually decreases as the liquefaction front moves through the deeper region of increasing shear strength.

Fig.4 illustrates the free surface horizontal displacement history for different magnitudes of the initial acceleration a_0. It can be seen that the predicted increase in the displacement amplitudes as the ground shaking progresses is relatively small. It should be noted, however, that in the model applied here no soil strength loss takes place once the ground liquefaction has occurred, and the residual (i.e. at $\overline{p} = 0$) shear moduli are used to model the post-liquefaction behaviour of the soil.

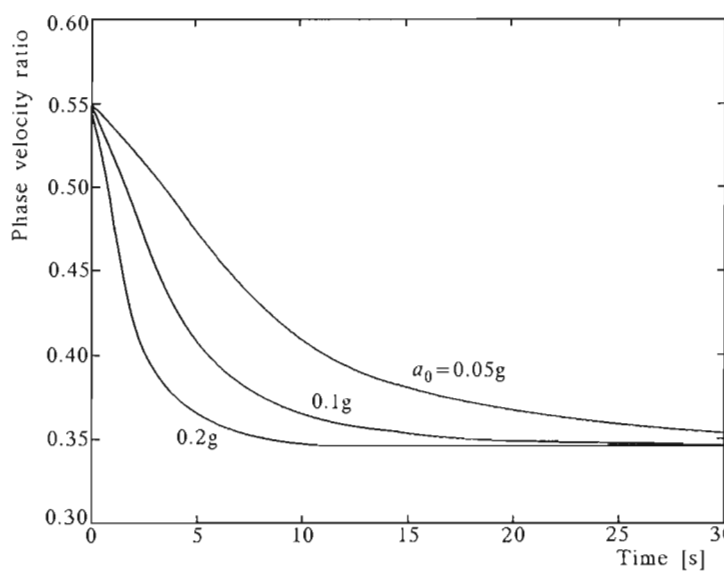

Fig. 5. Variation of Love wave phase velocity with time for different initial free surface acceleration amplitudes a_0

Finally, Fig.5 shows the variation of the wave phase velocity with time and demonstrates the progressive weakening of the sand layer as a whole. The Love wave phase velocity $c = \omega/k$ is normalised with respect to the shear wave velocity in the underlying half-space $c_2 = \sqrt{G_r/\rho_r}$, i.e. the ratios c/c_2 are plotted in the figure.

5. Conclusions

In this paper the problem of dynamic response of a water-saturated sand layer to cyclic loading induced by a Love wave passage has been treated. The analysis of the pore water pressure generation and soil liquefaction phenomena has been pursued by applying a compaction theory of saturated granular materials. The results of numerical simulations, carried out for data corresponding to a loose sand, have shown that strong ground motions of magnitudes typical for earthquakes can give rise to extensive ground liquefaction in a saturated sand deposit within several seconds following the start of shaking. Compared to the related problem of Rayleigh waves propagation, the pore pressure generation and liquefaction phenomena due to the Love waves action develop more regularly, without significant changes in time rates during an earthquake. Owing to the relative simplicity of the adopted constitutive laws, and the transformation of the plane wave propagation problem into a one-dimensional space problem, the proposed method avoids many numerical difficulties inherent in more complex approaches, such as plasticity models. Therefore, the presented method provides a useful theoretical tool for assessing the liquefaction potential of saturated sand deposits, which can be applied not only in the case of seismic loading, but also in other engineering problems involving dynamic loads.

Acknowledgement

The author thanks Prof. L.W. Morland of the University of East Anglia in Norwich for constructive comments that helped to improve the final version of the paper.

A. Appendix

The plane wave propagation problem has been solved numerically by the use of an incremental step-by-step method in time and the finite element

method in space variables. The problem discussed can be transformed into a one-dimensional space problem by applying a method proposed by Lysmer (1970), and followed by Sawicki and Staroszczyk (1995) and Staroszczyk (1996) to analyse the propagation of Rayleigh waves. In Lysmer's method the plane domain is first discretized by using a mesh of rectangular finite elements, and then, by considering a limit case of zero element horizontal spacings, the problem is subsequently reduced to a one-dimensional space problem.

In this paper we apply a more straightforward approach, in which the problem is transformed to an equation in one space variable before the discretization is carried out. To this end let consider the momentum equation in the x_2-direction

$$\frac{\partial \sigma_{21}}{\partial x_1} + \frac{\partial \sigma_{23}}{\partial x_3} = \rho \frac{\partial^2 u}{\partial t^2} \tag{A.1}$$

where ρ is the medium density. By virtue of Eq (2.26), the shear stresses are $\sigma_{21} = G(\partial u/\partial x_1)$ and $\sigma_{23} = G(\partial u/\partial x_3)$, and hence Eq (A.1) leads to the relation

$$G\Big(\frac{\partial^2 u}{\partial x_1^2} + \frac{\partial^2 u}{\partial x_3^2}\Big) = \rho \frac{\partial^2 u}{\partial t^2} \tag{A.2}$$

On account of the assumed form of the displacement field (2.1), determining the $\partial u/\partial x_1$ and $\partial u/\partial t$ derivatives, the latter equation becomes

$$(k^2 G - \omega^2 \rho) u_0 = G \frac{\partial^2 u_0}{\partial x_3^2} \tag{A.3}$$

The function $u_0(x_3)$ is approximated by means of the formula

$$u_0(x_3) \approx \Phi_i(x_3) w_i \tag{A.4}$$

where Φ_i $(i = 1, \ldots, N)$ are shape (interpolation) functions, w_i are nodal displacement amplitudes, and N is the total number of discrete points. Now, Eq (A.3) can be transformed into a set of algebraic equations by applying the weighted residual (Galerkin) method, which allows the adopted approximation to satisfy Eq (A.3) in an integral mean sense. Accordingly, by premultiplying Eq (A.3) by Φ_j and integrating over the spatial domain Ω, one obtains (after the use of Green's theorem and insertion of the boundary conditions (2.2)) the following matrix relation

$$\big(\mathbf{K} - \omega^2 \mathbf{M}\big)\boldsymbol{w} = \mathbf{0} \tag{A.5}$$

where $\boldsymbol{w} = [w_1, \ldots, w_i, \ldots, w_N]^\top$. The entries in the stiffness and mass matrices, $\mathbf{K}$ and $\mathbf{M}$ respectively, are defined by

$$K_{ij} = \int_{\Omega} G(x_3)\left(k^2 \Phi_i \Phi_j + \frac{d\Phi_i}{dx_3}\frac{d\Phi_j}{dx_3}\right) dx_3 \qquad M_{ij} = \int_{\Omega} \rho(x_3)\Phi_i \Phi_j \, dx_3 \tag{A.6}$$

In the case of linear shape functions Φ_i, the element stiffness and mass matrices are

$$\mathbf{K}_j^e = G_j \begin{bmatrix} \frac{k^2 b_j}{3} + \frac{1}{b_j} & \frac{k^2 b_j}{6} - \frac{1}{b_j} \\ \frac{k^2 b_j}{6} - \frac{1}{b_j} & \frac{k^2 b_j}{3} + \frac{1}{b_j} \end{bmatrix} \qquad \mathbf{M}_j^e = \frac{\rho_j b_j}{6} \begin{bmatrix} 2 & 1 \\ 1 & 2 \end{bmatrix} \tag{A.7}$$

where G_j and ρ_j are the shear modulus and density in the jth element, and b_j is the element size.

Eq (A.5) defines the generalised eigenvalue problem for the real and symmetric matrices $\mathbf{K}$ and $\mathbf{M}$. Since in the problem considered the angular frequency ω is a prescribed parameter, the eigenvalue problem has to be solved iteratively in order to determine the wavenumber k entering the stiffness matrix $\mathbf{K}$. From among the real eigenvectors $\boldsymbol{w}_i$, the one related to the lowest eigenvalue is chosen as that corresponding to the propagating surface wave. This fundamental wave mode is then normalised with respect to a selected wave parameter (such as the free surface acceleration amplitude, total wave energy, etc.), which determines the elastic shear strains, necessary to evaluate the compaction strain and pore pressure rates in the current strain and stress state, as described in Section 3.

References

1. ACHENBACH J.D., 1973, *Wave Propagation in Elastic Solids*, North-Holland, Amsterdam
2. BAŽANT Z.P., KRIZEK R.J., 1976, Endochronic Constitutive Law for Liquefaction of Sand, *Proc. ASCE, J. Mech. Engng Div.*, **102**, 225-238
3. BAŽANT Z.P., KRIZEK R.J., SHIEH, C.L., 1983, Histeretic Endochronic Theory for Sand, *J. Engng Mech. – ASCE*, **109**, 1073-1095
4. BERRILL J.B., DAVIS R.O., 1985, Energy Dissipation and Seismic Liquefaction of Sands: Revised Model, *Soils and Found.*, **25**, 106-118

5. BIOT M.A., WILLIS D.G., 1957, The Elastic Coefficients of the Theory of Consolidation, *J. Appl. Mech.*, **10**, 594-601

6. CHAKRABORTY S.K., DEY S., 1982, The Propagation of Love Waves in Water-Saturated Soil Underlain by a Heterogeneous Elastic Medium, *Acta Mech.*, **44**, 169-176

7. CHATTOPADHYAY A., CHAKRABORTY M., KUSHWAHA V., 1986, On the Dispersion Equation of Love Waves in a Porous Layer, *Acta Mech.*, **58**, 125-136

8. DERESIEWICZ H., 1961, The Effect of Boundaries on Wave Propagation in a Liquid-Filled Porous Solid, II. Love Waves in a Porous Layer, *Bull. Seism. Soc. Am.*, **51**, 51-59

9. EWING W.M., JARDETZKY W.S., PRESS F., 1957, *Elastic Waves in Layered Media*, McGraw-Hill, New York

10. FINN W.D., LEE K.W., MARTIN G.R., 1977, An Effective Stress Model for Liquefaction, *Proc. ASCE, J. Geotech. Engng Div.*, **103**, 517-533

11. GAZETAS G., YEGIAN M.K., 1979, Shear and Rayleigh Waves in Soil Mechanics, *Proc. ASCE, J. Geotech. Engng Div.*, **105**, 1455-1470

12. GHABOUSSI J., DIKMEN S.U., 1978, Liquefaction Analysis of Horizontally Layered Sands, *Proc. ASCE, J. Geotech. Engng Div.*, **104**, 341-356

13. KOŃCZAK Z., 1989, The Propagation of Love Waves in a Fluid-Saturated Porous Anisotropic Layer, *Acta Mech.*, **79**, 155-168

14. LAW K.T., CAO Y.L., HE G.N., 1990, An Energy Approach for Assessing Seismic Liquefaction Potential, *Can. Geotech. J.*, **27**, 320-329

15. LYSMER J., 1970, Lumped Mass Method for Rayleigh Waves, *Bull. Seism. Soc. Am.*, **60**, 89-104

16. MARTIN G.R., FINN W.D.L., SEED H.B., 1975, Fundamentals of Liquefaction under Cyclic Loading, *Proc. ASCE, J. Geotech. Engng Div.*, **101**, 423-438

17. MARTIN P.P., SEED H.B., 1979, Simplified Procedure for Effective Stress Analysis of Ground Response, *Proc. ASCE, J. Geotech. Engng Div.*, **105**, 739-758

18. MORLAND L.W., 1993, Compaction and Shear Settlement of Granular Materials, *J. Mech. Phys. Solids*, **41**, 507-530

19. MORLAND L.W., SAWICKI A., 1983, A Mixture Model for the Compaction of Saturated Sand, *Mech. Mat.*, **2**, 217-231

20. MORLAND L.W., SAWICKI A., 1985, A Model for Compaction and Shear Hysteresis in Saturated Granular Materials, *J. Mech. Phys. Solids*, **33**, 1-24

21. MORLAND L.W., SAWICKI A., MILNE P.C., 1993, Uni-Axial Compaction of a Granular Material, *J. Mech. Phys. Solids*, **41**, 1755-1779

22. MORLAND L.W., STAROSZCZYK R., 1998, Uni-Axial Wave Propagation and Pore Pressure Generation in Fluid Saturated Sands Exhibiting Irreversible Compaction, *Int. J. Num. Anal. Meth. Geomech.*, in press

23. NEMAT-NASSER S., SHOKOOH A., 1979, A Unified Approach to Densification and Liquefaction of Cohesionless Sand in Cyclic Shearing, *Can. Geotech. J.*, **16**, 659-678

24. PANDE G.N., ZIENKIEWICZ O.C. (EDIT.), 1982, *Soil Mechanics – Transient and Cyclic Loads*, Wiley, Chichester

25. SAWICKI A., MORLAND L.W., 1985, Pore Pressure Generation in a Saturated Sand Layer Subjected to a Cyclic Horizontal Acceleration at its Base, *J. Mech. Phys. Solids*, **33**, 545-559

26. SAWICKI A., STAROSZCZYK R., 1995, Development of Ground Liquefaction Due to Surface Waves, *Arch. Mech.*, **47**, 557-576

27. SCHAEFFER D.G., 1990, Mathematical Issues in the Continuum Formulation of Slow Granular Flow, In: Joseph D.D. and Schaeffer D.G. (edit.) *Two Phase Flows and Waves*, 118-129, Springer, New York

28. SEED H.B., MARTIN P.P., LYSMER J., 1976, Pore-Water Pressure Changes During Soil Liquefaction, *Proc. ASCE, J. Geotech. Engng Div.*, **102**, 323-346

29. STAROSZCZYK R., 1996, Pore Pressure Generation and Liquefaction in Saturated Sands Due to the Propagation of Surface Waves, *Acta Geophys. Pol.*, **44**, 195-218

30. STUDER J., KOK L., 1980, Blast-Induced Excess Porewater Pressure and Liquefaction. Experience and Application, *Proc. Int. Symp. on Soil under Cyclic and Transient Loading*, Swansea, Balkema, 581-593

31. SYVITSKI J., SCHAFER C., 1990, *ADFEX – Environmental Impact Statement*, Geological Survey of Canada, Dartmouth

32. VALANIS K.C., 1971, A Theory of Viscoplasticity without a Yield Surface. I. General Theory, *Arch. Mech.*, **23**, 517-533

33. VALANIS K.C., PETERS J.F., 1991, An Endochronic Plasticity Theory with Shear-Volumetric Coupling, *Int. J. Num. Anal. Meth. Geomech.*, **15**, 77-102

34. VALANIS K.C., READ H.E., 1982, A New Endochronic Plasticity Model for Soils, In: Pande G.N., Zienkiewicz O.C. (edit.) *Soil Mechanics – Transient and Cyclic Loads*, 375-417, Wiley, Chichester

35. ZIENKIEWICZ O.C., LEUNG K.H., HINTON E., CHANG C.T., 1982, Liquefaction and Permanent Deformation under Dynamic Conditions – Numerical Solution and Constitutive Relations, In: Pande G.N. and Zienkiewicz O.C. (edit.) *Soil Mechanics – Transient and Cyclic Loads*, 71-103, Wiley, Chichester

Upłynnienie gruntu w warstwie nawodnionego piasku wywołane propagacją fal Love'a

Streszczenie

Praca poświęcona jest płaskiemu zagadnieniu propagacji fal Love'a w warstwie piasku nasyconego wodą, znajdującej się na półprzestrzeni ośrodka sprężystego. Obciążenia dynamiczne spowodowane przejściem fali wywołują nieodwracalne odkształcenia w szkielecie gruntowym, które są przyczyną zwiększenia ciśnienia w wodzie wypełniającej pory ośrodka i tym samym zmniejszenia naprężeń efektywnych w gruncie, co w końcowym przypadku może prowadzić do upłynnienia podłoża. Proces generacji ciśnień porowych jest analizowany na bazie teorii zagęszczania nawodnionych ośrodków granulowanych. Wyniki obliczeń numerycznych, przeprowadzonych w oparciu o metodę elementów skończonych, ilustrują ewolucję ciśnień porowych, rozwój strefy upłynnienia w podłożu oraz zmiany w czasie przemieszczeń powierzchni swobodnej warstwy.

Manuscript received November 25, 1997; accepted for print February 23, 1998